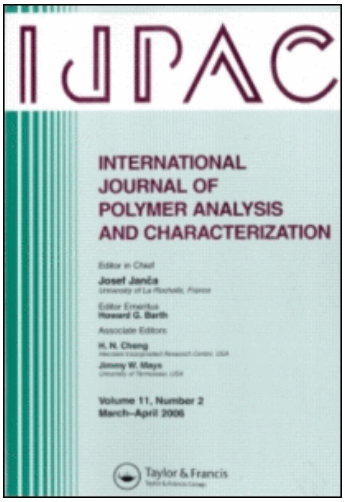


**International Journal of Polymer Analysis and Characterization**
Publication details, including instructions for authors and subscription information:
http://www.informaworld.com/smpp/title~content=t713646643

# Characterization and Degradation of Hydroxyl-Containing Fluorinated Poly(siloxane imide)

G. P. Wang[a]; T. C. Chang[a]; Y. S. Hong[a]; Y. S. Chiu[b]
[a] Department of Applied Chemistry, Chung Cheng Institute of Technology, NDU, Tahsi, Taoyuan, Taiwan, Republic of China [b] Chemical Systems Research Division, Chung Shan Institute of Science and Technology, Taoyuan, Taiwan, Republic of China

Online publication date: 27 October 2010

**To cite this Article** Wang, G. P. , Chang, T. C. , Hong, Y. S. and Chiu, Y. S.(2002) 'Characterization and Degradation of Hydroxyl-Containing Fluorinated Poly(siloxane imide)', International Journal of Polymer Analysis and Characterization, 7: 3, 227 — 243
**To link to this Article: DOI:** 10.1080/10236660211185
**URL:** http://dx.doi.org/10.1080/10236660211185

International Journal of Polymer Anal. Charact., 7: 227–243, 2002

1023-666X/02 $12.00+.00

# *Characterization and Degradation of Hydroxyl-Containing Fluorinated Poly(siloxane imide)*

**G. P. Wang, T. C. Chang, and Y. S. Hong**
Department of Applied Chemistry, Chung Cheng Institute of Technology, NDU, Tahsi, Taoyuan, Taiwan, Republic of China

**Y. S. Chiu**
Chemical Systems Research Division, Chung Shan Institute of Science and Technology, Lungtan, Taoyuan, Taiwan, Republic of China



*The hydroxyl-containing fluorinated poly(siloxane imide)s (FPSIs) were synthesized by polycondensation reaction of 4,4′-(hexafluoroisopropylidene) diphthalic anhydride (6FDA) with 2,2′-bis(3-amino-4-hydroxyphenyl) hexafluoropropane (AHHFP) and 1,3-bis(3-aminopropyl) tetramethyldisiloxane (APrTMDS). Infrared (IR), differential scanning calorimetry (DSC), thermogravimetric analysis (TGA), and $^{13}$C-nuclear magnetic resonance (NMR) spectroscopy were used to characterize the structure of FPSI copolymers. The thermal and thermooxidative degradation of FPSI copolymers was studied by thermogravimetry and compared with unmodified fluorinated polyimide. The dynamics of the FPSI copolymers were also investigated by proton spin-spin relaxation measurements.*

*Keywords*: Fluorinated poly(siloxane imide); Thermooxidative degradation; Nuclear magnetic resonance; Spin-spin relaxation

Received 30 November 2000; accepted 19 January 2001.

We thank Miss S. Y. Fang (Tsing Hua University) for help in the NMR measurements and Mr. Y. C. Lin (Chung Shan Institute of Science and Technology) for help in the TGA measurements.

Address correspondence to T. C. Chang, Department of Applied Chemistry, Chung Cheng Institute of Technology, NDU, Tahsi, Taoyuan, Taiwan 335, Republic of China.

Polyimide consists of organic dianhydride and a diamine. It is widely used for applications that require a high degree of thermal stability, low dielectric constant, excellent mechanical properties, and chemical resistance. However, it is insoluble in most organic solvents. Nevertheless, its precursor, polyamic acid, can easily be processed by spin coating or the air-brush method. When fluorine atoms are incorporated into the PI structure some additional properties are also improved, for example water sorption, the dilectric constant, and optical losses are all reduced[1]. Therefore, fluorinated polyimide has attracted attention for applications in gas separation[2], pervaporation[3], optics[4–7], interlayer dielectric films[8–9], and photoresist[10–12]. However, fluorinated polyimide is also a attractive polymeric film material because of its good film-forming properties. In spite of these unique characteristics, the sensor application studies with polyimide and fluorinated polyimide have rarely been reported[13–17].

Polymer, with glassy and crystalline domains exhibit low vapor permeability and are not good candidates for surface acoustics wave (SAW) coatings. Therefore, polymer coatings with low glass-transition temperature $T_g$ are preferable for SAW devices. Polysiloxanes are chemically stable and have very low $T_g$, imparting optimum viscoelastic properties for rapid vapor sorption. They are rarely used in chemical sensor systems[18,19]. In addition to having favorable permeation properties, the polymer must be soluble in a volatile solvent and exhibit stable, well-formed coating. In a previous paper, we characterized the dynamics and stability of the soluble polyimide. We found that the rigid imide segments restricted the motion of the polysiloxane chains, and the flexible polysiloxane segments enchanced the stability of imide segments[20]. Furthermore, soluble polyimide with hydroxyl group can be phosphorylated, and the values of $E_a$ in thermal degradation decreased with increasing phosphorus condtant[21].

Kuckertz first reported the flexible siloxane dimmer incorporated into polyimide[22]. Furthermore, Clair et al., reported on the synthesis of fluorinated polyimide from 4,4′-(hexafluoroisopropylidene)diphthalic anhydride (6FDA)[23]. In this article, fluorinated poly(siloxane imide) (FPSI) with hydroxy groups are synthesized from 2,2′-bis(3,4-dicarboxyphenyl) hexafluoropropane anhydride (6FDA), 2,2′-bis(3-amino-4-hydroxyphenyl)hexafluropropane (BAPAF) and 1,3-bis(3-aminopropyl) tetramethyldisiloxane (APrTMDS). IR, $^{13}C$-, $^{29}Si$-NMR, DSC, and TGA are used to characterize FPSI. To understand the dynamics of the imide and APrTMDS segment, we have measured proton relaxation times respective in their segments. Additionally, the effect of APrTMDS content on the degradation of FPSI copolymers both in $N_2$ and air has been also investigated.

## EXPERIMENTAL

### Materials

4,4′-(Hexafluoroisopropylidene)diphthalic anhydride (6FDA, Chris) was subjected to a general purification method. 2,2′-bis(3-amino-4-hydroxy phenyl)hexafluoropropane (AHHFP, Chris) and 1,3-bis(3-aminopropyl) tetramethyldisiloxane (APrTMDS, TCI) were used without purification. *N*,*N*-dimethyl-acetamide (DMAc, Aldrich) was distilled under a vacuum, and toluene (Aldrich) was dried over molecular sieve 4 Å.

### Synthesis of Polyimides

Fluorinated polyimides were prepared through a conventional two-step process (Scheme 1). The feed compositions of the various fluorinated polyimides are listed in Table I. Hydroxyl-containing fluorinated polyimide FPI was prepared by the solution imidization method with a 3:1 (v/v) DMAc/toluene mixture, and polymerization was conducted under nitrogen with the concentration of 15% solids by weight in a cosolvent. A stoichiometric amount of the AHHFP diamine (0.02 mol) was added to a 3/1 (v/v) DMAc/toluene solution (15 wt%) of 6FDA (0.02 mol). After the mixture stirred at room temperature for 24 h, it was cast in a mold and then heated at 160°C for 24 h. The obtained film was ground to powder, and dried under a vacuum at 80°C for 8 h. A yellow brown solid hydroxyl-containing fluorinated polyimide (FPI) was obtained and characterized by IR, NMR, DSC, and TGA.

The hydroxyl-containing fluorinated poly(siloxane imide)s FPSI-20, FPSI-35, FPSI-50, and FPSI-75 were prepared under different feed compositions. A typical synthesis was as follows. Siloxane monomer



**TABLE I** Experimental conditions for polyimides synthesis.

| Polyimides | 6F-DA (mol) | AHHFP (mol) | APrTMDS (mol) | DMAc/Toluene 3/1 (ml) |
|---|---|---|---|---|
| FPI | 0.020 | 0.020 | 0 | 91 |
| FPSI-20 | 0.020 | 0.016 | 0.004 | 88 |
| FPSI-35 | 0.020 | 0.013 | 0.007 | 86 |
| FPSI-50 | 0.020 | 0.010 | 0.010 | 84 |
| FPSI-75 | 0.020 | 0.005 | 0.015 | 80 |
| FPSI-100 | 0.020 | 0 | 0.020 | 76 |

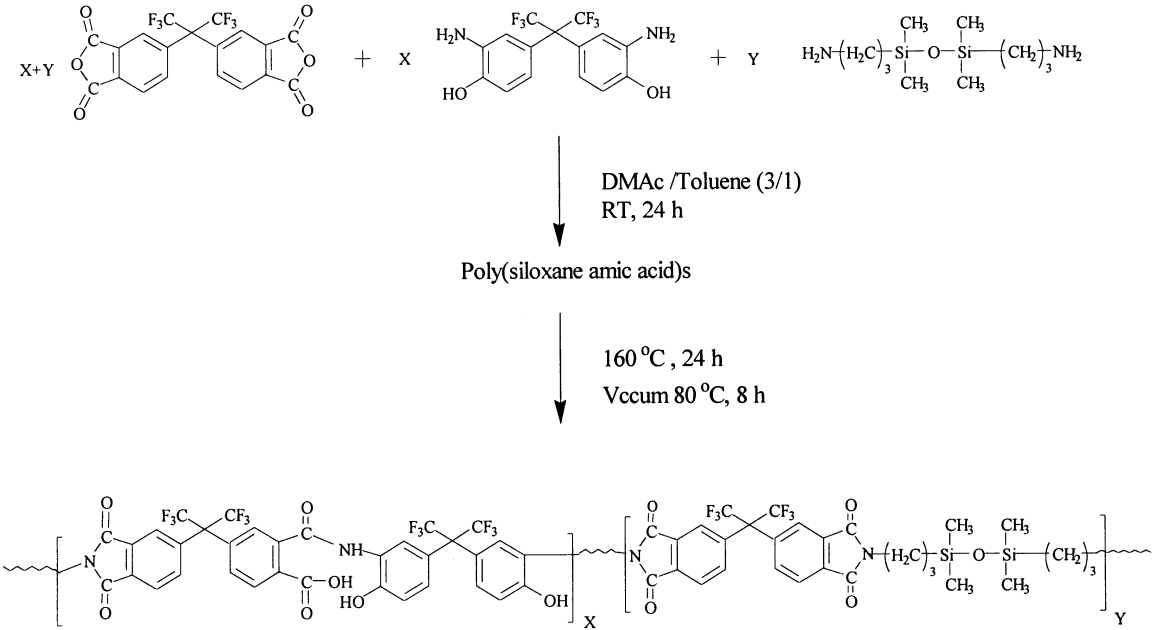


Y=0, Hydroxyl-containing fluorinated polyimide, PI
X=0, fluorinated Poly(siloxane imide), PSI-100
X≠0; Y≠0, Hydroxyl-containing fluorinated poly(siloxane imide)

**SCHEME 1.**

APrTMDS (0.01 mol) was first slowly added to a stirring solution of 6FDA (0.02 mol) and cosolvent (DMAc:toluene = 3:1), effectively capping the disiloxane through reaction of its amine end groups. The aromatic diamine AHHFP (0.01 mol) was then gradually added as a solution to the free dianhydride and anhydride-capped disiloxane. Thereafter, the experimental process was similar to that for FPI. The hydroxyl-containing fluorinated poly(siloxane imide) FPSI-50 was then obtained, where 50 denotes mol % of APrTMDS based on the mole of the diamine monomer (AHHFP and APrTMDS).

Fluorinated poly(siloxane imide) FPSI-100 was prepared under similar experimental conditions as FPI by reacting 6FDA (0.02 mol) with APrTMDS (0.02 mol).

### Characterization of the Polyimides

Infrared spectra of samples dispersed in dry KBr pellets were recorded between 4000 and 550 $cm^{-1}$ on a Bomen DA 3.002 FTIR spectrometer. The $^{29}Si$- and $^{13}C$-nuclear magnetic resonance (NMR) spectra of the polyimides were determined (Bruker MSL-400) by using the cross-polarization combined with magic angle spinning (CP/MAS) technique. Proton spin-spin relaxation time ($T_2$) was measured at room temperature via solid-state $^{13}C$ NMR using the pulse sequence described by Tékély[24]. Differential scanning calorimetry (DSC) was conducted in a Perkin Elmer 7 unit. The characteristics and kinetics of degradation of fluorinated polyimides were measured by a Perkin-Elmer TGA-7 at heating rate of 10°C/min under air and nitrogen. The sample weight was about 10 mg, and the gas flow rate was kept at 100 mL/min.



## RESULTS AND DISCUSSION

### Characterization

Figure 1 shows the IR spectra of fluorinated polyimides containing various proportions of siloxane segments. The hydroxyl-containing fluorinated polyimide FPI (figure 1A) presents the characteristic imide peaks at 1786 $cm^{-1}$ (imide C=O symmetric stretching), 1722 $cm^{-1}$ (imide C=O asymmetric stretching), 1376 $cm^{-1}$ (imide C-N stretching) and 722 $cm^{-1}$ (imide ring deformation)[20]. These characteristic absorption peaks of imide groups are also observed in the spectra of FPSIs [figure 1 (B–F)]. However, the intensities of the amide absorptions (1611 $cm^{-1}$ and 1516 $cm^{-1}$) and hydroxyl group (3400–3200 $cm^{-1}$) decrease with increasing disiloxane content,

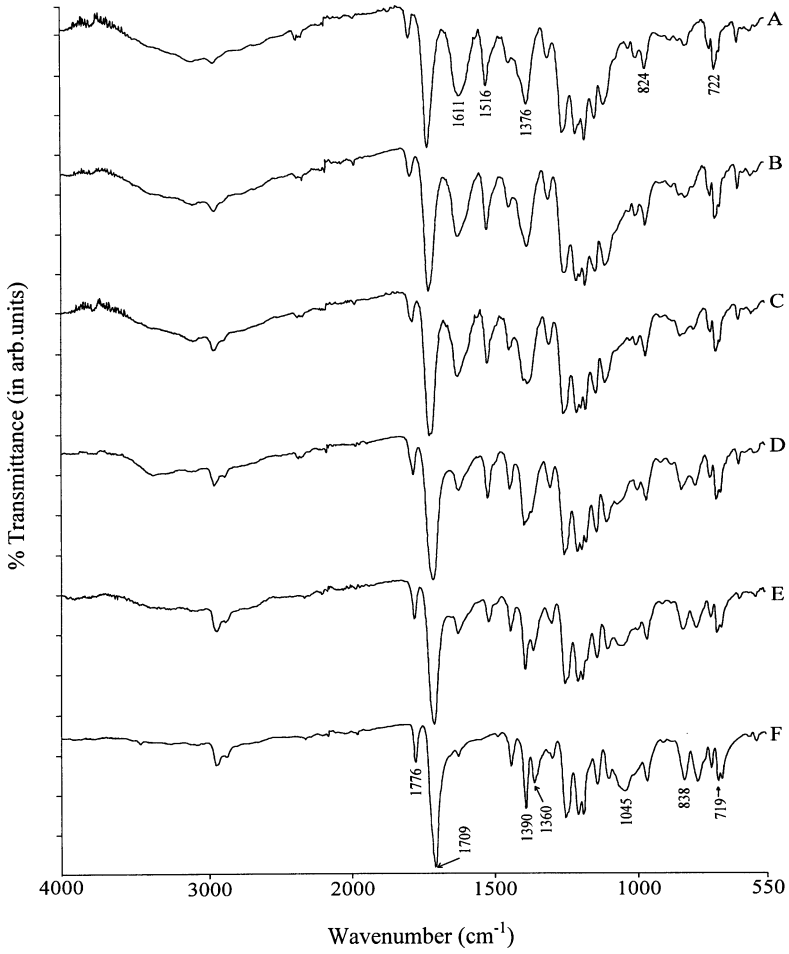


**FIGURE 1** Infrared spectra of the various fluorinated polyimides (A) FPI, (B) FPSI-25, (C) FPSI-35, (D) FPSI-50, (E) FPSI-75, and (F) FPSI-100.

whereas the intensity of the Si-O-Si absorption (1045 $cm^{-1}$) increases. The results reveal that the flexible APrTMDS enhances the degree of the imidization.

The $^{13}C$ CP/MAS NMR spectra of polyimides are shown in Figure 2. A set of peak for FPI (Figure 2A) is observed at 166, 155, 140–118 and 64 arising from imide carbonyl, aryl carbons with hydroxyl groups, various aromatic carbons and trifluoromethyl

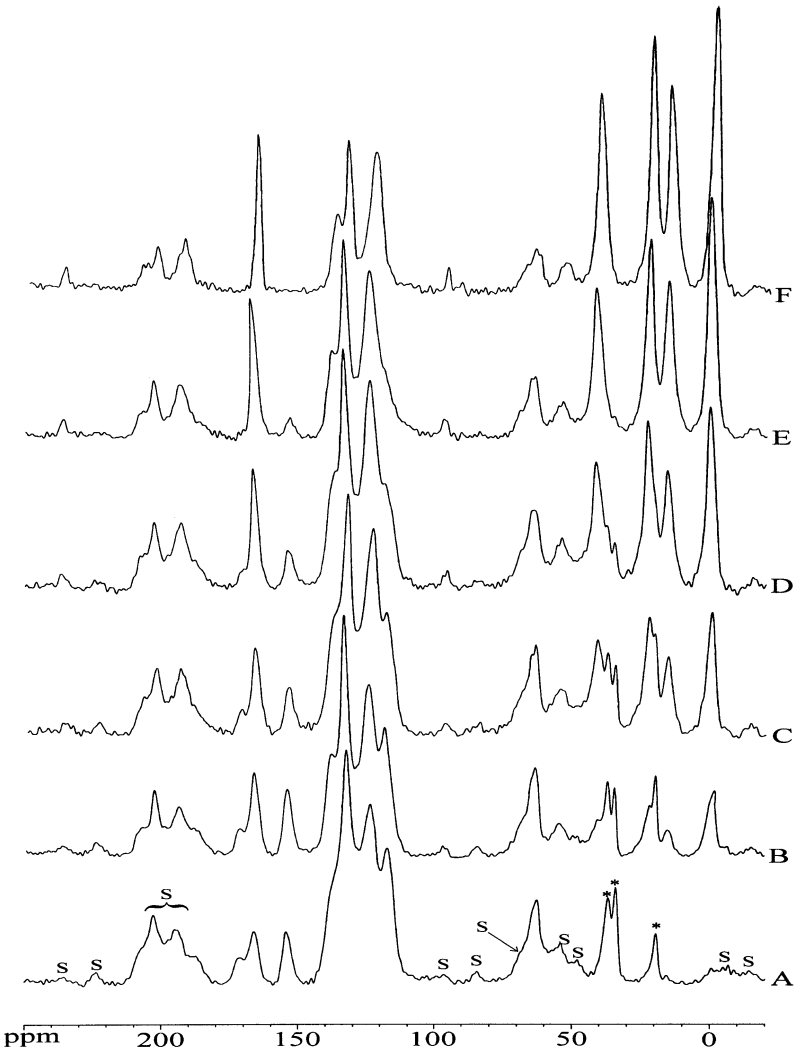


**FIGURE 2** $^{13}C$ CP/MAS NMR spectra of (A) FPI, (B) FPSI-25, (C) FPSI-35, (D) FPSI-50, (E) FPSI-75 and (F) FPSI-100 (S: sideband, *: solvent peak).

carbons, respectively[20]. The $^{13}C$ CP/MAS NMR spectra of hydroxyl-containing FPSIs [Figure 2 (B–E)] are nearly identical. The intensities of the peaks at 154 and 67 ppm decrease with increasing

disiloxane content, whereas those at around 41, 22, 16, and 0 ppm increase. This latter set of chemical shifts is then due to APrTMDS segments, which correspond to $-NCH_2-$, $-CH_2-$, $-CH_2Si-$ and $-SiCH_3$, respectively. Therefore, $^{13}C$ CP/MAS NMR spectrum of FPSI-100 (Figure 2F) shows only the characteristic peaks of imide carbonyl, various aromatic carbons, quartet carbons, and APrTMDS segments. The resonances at 38, 35, and 20 ppm are solvent peaks (DMAc) and decrease with increasing disiloxane content. The result implies that the interaction between hydroxyl-containing fluorinated imide segments with DMAc is decreased. Therefore, the APrTMDS can modify the acidity of the FPI polymer. However, the chemical shifts of $^{29}Si$ CP/MAS NMR spectra for FPSIs are around 8 ppm, and the

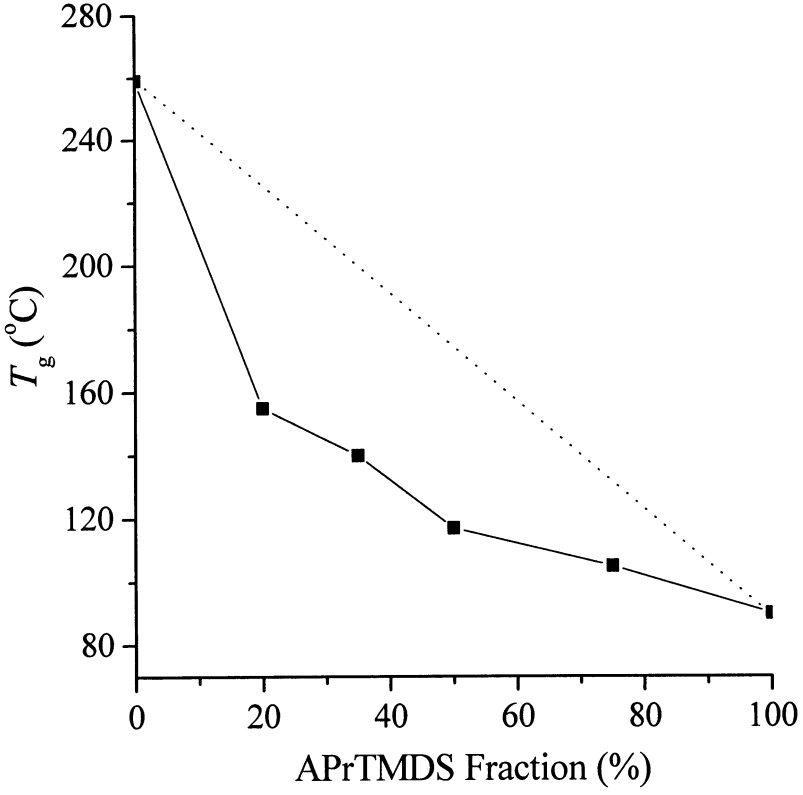


**FIGURE 3** Relationship between glass-transition temperature and molar fraction of APrTMDS for FPSIs.

peak widths (~700 Hz) are independent of the APrTMDS content. It suggests that the silicons in FPSIs have a similar electronic environment.

## Thermal Analysis

The glass-transition temperatures ($T_g$) of the FPI in this work is 259°C. However, the values of $T_g$ of FPSIs decrease with the enhancement of APrTMDS to around 90°C (Figure 3). Apparently, with the addition of the flexible APrTMDS as a segment in polyimide structure, a lowering of $T_g$ is expected. However, the lower concave from the $T_g$ diagram for miscible blends implies that the intermolecular interaction,

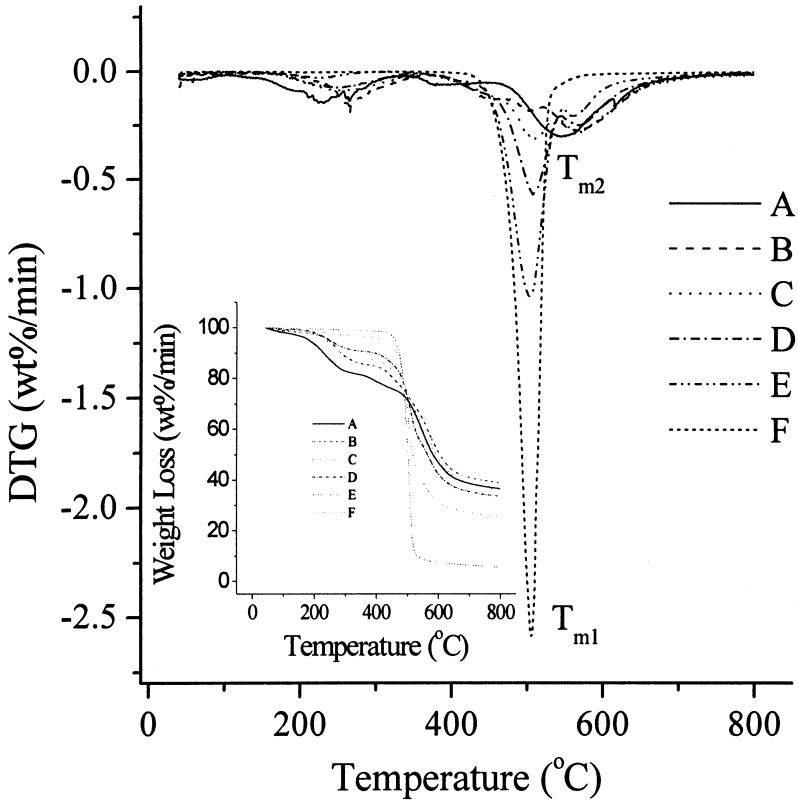


**FIGURE 4** DTG and TGA thermograms of (A) FPI, (B) FPSI-25, (C) FPSI-35, (D) FPSI-50, (E) FPSI-75 and (F) FPSI-100 in $N_2$ at the heating rate 10°C/min.

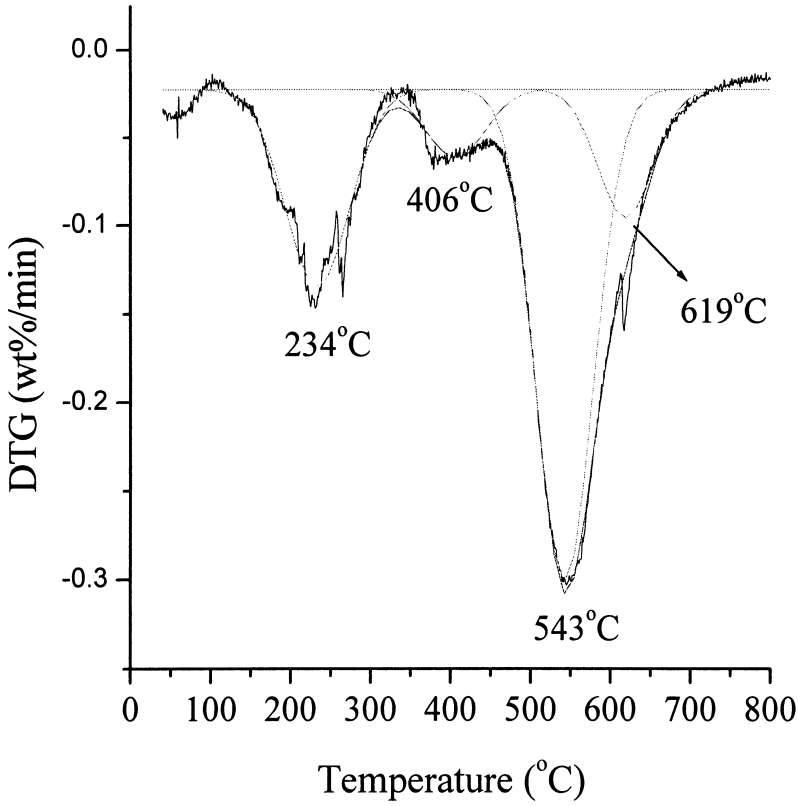


**FIGURE 5** The deconvoluted DTG curve of FPI at thermal degradation (10°C/min).

such as hydrogen bonding, reduced as APrTMDS is added[25]. Therefore, the gas diffusion in the FPSI could be increased as APrTMDS is incorporated into polyimides.

Thermal stability of fluorinated polyimides is evaluated from TGA. Figure 4 shows TGA and DTG curves of the fluorinated polyimides under nitrogen at a heating rate of 10°C/min. FPI degrades by a three-step process (Figure 4A), and is virtually destroyed at 800°C. However, the deconvoluted DTG curve of FPI (Figure 5) shows mainly a four-step process. The peak temperature of each degradation is about 234°, 406°, 543°, and 619°C, respectively. The weight loss in the first stage ($\sim$112 wt%) is subjected to the imidization of amic acid. The second step (3.6 wt%) can be attributed to the scissions of F species from 6F

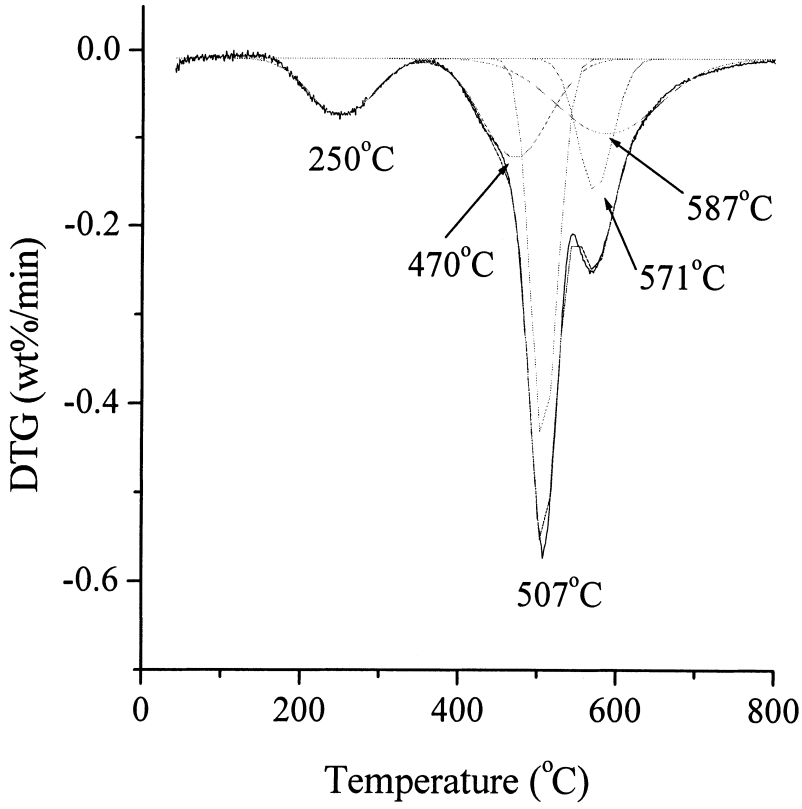


**FIGURE 6** The deconvoluted DTG curve of FPSI-50 at thermal degradation (10°C/min).



connecting linkages and of CO from unreacted anhydride end group[26], the third step (25.1 wt%) to the scissions at C-N imide linkage[26], and the most stable step (6.3 wt%) to random scission within the aromatic ring.

The weight loss of the first stage in FPSIs decreases with increasing APrTMDS content [Figure 4 (B–F)], suggesting that APrTMDS is more easily imidized than that of AHHFP. The result is consistent with the IR spectrum. The deconvoluted DTG curves of FPSI-50 (Figure 6) clearly show evidence of the existence of APrTMDS segment degrade step (507°C), as observed from a comparison with Figure 5. Although, the rate of APrTMDS segment degradation ($dW/dt$) increases with increasing

disiloxane content, its peak temperature is independent of disiloxane content. Compared with the FPI, the enhanced degradation rate may be caused by thermal degradation beginning at the aliphatic *n*-propyl segments linking the APrTMDS segments to the 6FDA[20,21]. The results reveal that the thermal stability of FPSIs under nitrogen is less affected by the incorporation of the APrTMDS segments.

The TGA curves of FPSIs under air are shown in Figure 7. Continuous weight loss is observed below 350°C corresponding to the release of water and solvent under heating, which is evident of incomplete imidization. The char yield of FPSIs at 800°C in air is not

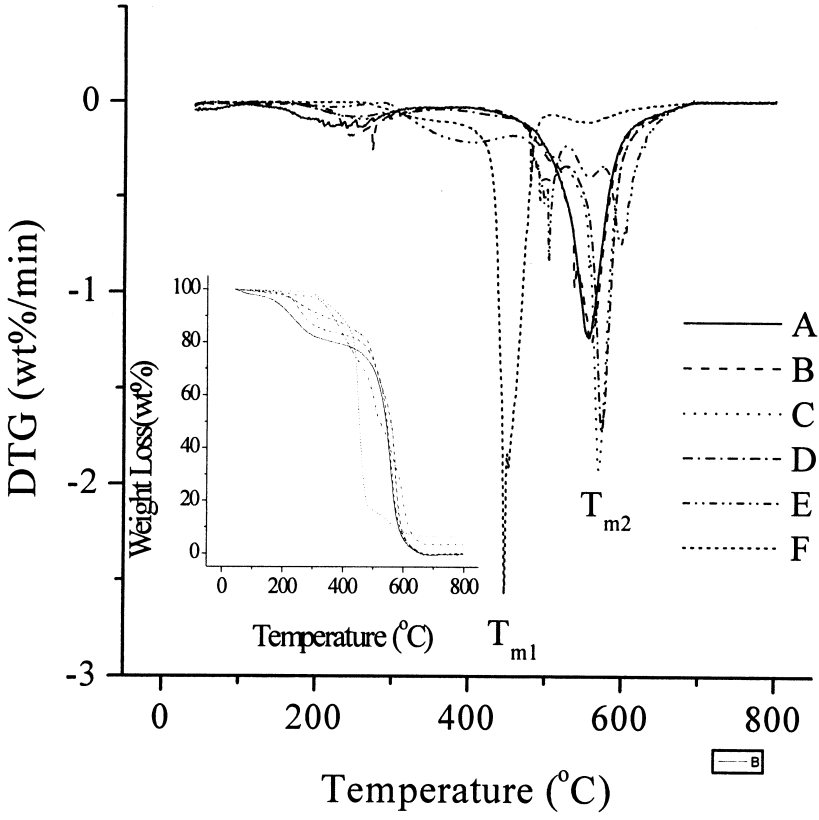


**FIGURE 7** DTG and TGA thermograms of (A) FPI, (B) FPSI-25, (C) FPSI-35, (D) FPSI-50, (B) FPSI-75 and (F) FPSI-100 under air at the heating rate 10°C/min.

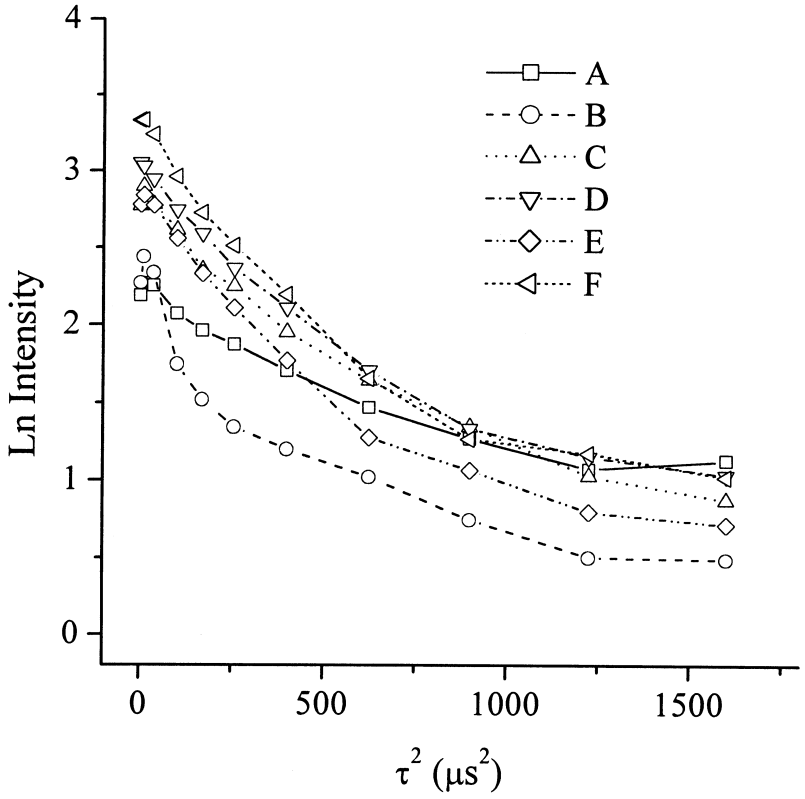


**FIGURE 8** Ln intensity of the $^{13}C$ CP/MAS spectra of the 167 ppm peak (imide carbonyl carbon) versus square of proton relaxation period $\tau^2$: (A) FPI, (B) FPSI-25, (C) FPSI-35, (D) FPSI-50, (E) FPSI-75, and (F) FPSI-100.

consistent with the calculated values (Table II). Note that the reduction of $Y_c$ suggests that some degraded silicon fluoride has evaporized[27]. The maximum rate temperature of weight loss of the disiloxane segments ($T_{m1}$) decreases with increasing APrTMDS content. However, the maximum rate temperatures of weight loss of the aromatic segments ($T_{m2}$) increase with increasing disiloxane content (Figure 7). In addition, the $Y_c$ value under air increases with increasing disiloxane content, whereas under $N_2$, it decreases. The results suggest that the incorporated APrTMDS segments enhance the thermooxidative stability of FPI.

**TABLE II** The characteristic parameters[a] of the degradation 10°C/min for various fluorinated polyimides.

| | $N_2$ | | | Air | | | |
|---|---|---|---|---|---|---|---|
| | | | | | | $Y_c$ (wt%) | |
| Polyimides | $T_{m1}$ (°C) | $T_{m2}$ (°C) | $Y_c$ (wt%) Exp. | $T_{m1}$ (°C) | $T_{m2}$ (°C) | Exp. | Cal. |
| FPI | – | 542 | 36.5 | – | 557 | 0.03 | – |
| FPSI-20 | 505 | 567 | 38.9 | 501 | 560 | 0.25 | 1.5 |
| FPSI-35 | 505 | 570 | 36.0 | 499 | 571 | 0.00 | 2.7 |
| FPSI-50 | 508 | 570 | 33.5 | 495 | 574 | 0.02 | 4.0 |
| FPSI-75 | 505 | 562 | 25.7 | 491 | 597 | 3.54 | 6.2 |
| FPSI-100 | 507 | – | 7.7 | 449 | – | 6.59 | 8.7 |

[a] $T_{m1}$, $T_{m2}$: Maximum polymer decomposition temperature; char yield at 800°C.



## Relaxation Property

The different chain mobility segments in FPSIs should result in different nuclear magnetic relaxation properties. Figure 8 shows the correlation between the logarithmic intensities of the 166 ppm peak (imide C=O) in $^{13}$C-NMR spectra of FPSIs and the square of the proton relaxation period ($\tau^2$). It is found that the carbons in imide segments exhibit two Gaussian spin-spin relaxations expressed as $I = \exp[-(\tau/T_2)^2/2]$ with two different relaxation times, indicating that the imide carbonyl carbons can be found in two different environments[24]. The slopes of straight lines yield the spin-spin relaxation times $T_2$ (fast)

**TABLE III** Proton spin-spin relaxation time ($T_2$) of polyimides.

| | PI phase | | APrTMDS | |
|---|---|---|---|---|
| Polyimides | $T_2$/μs | $T_2$/μs | $T_2$/μs | $T_2$/μs |
| FPI | 24.3(58.7)[a] | 72.5(41.3) | – | – |
| FPSI-20 | 11.3(78.4) | 52.9(21.6) | 12.5(72.6) | 54.9(27.4) |
| FPSI-35 | 17.4(63.4) | 38.7(36.6) | 19.0(68.3) | 46.5(31.7) |
| FPSI-50 | 17.8(74.3) | 48.7(25.7) | 18.7(73.2) | 54.3(26.8) |
| FPSI-75 | 17.6(75.5) | 45.1(24.5) | 18.8(63.8) | 42.8(36.2) |
| FPSI-100 | 16.0(82.9) | 53.4(17.1) | 18.3(65.7) | 41.3(34.3) |

[a]Numbers in parentheses are fractions (%) of different domains in polyimides.

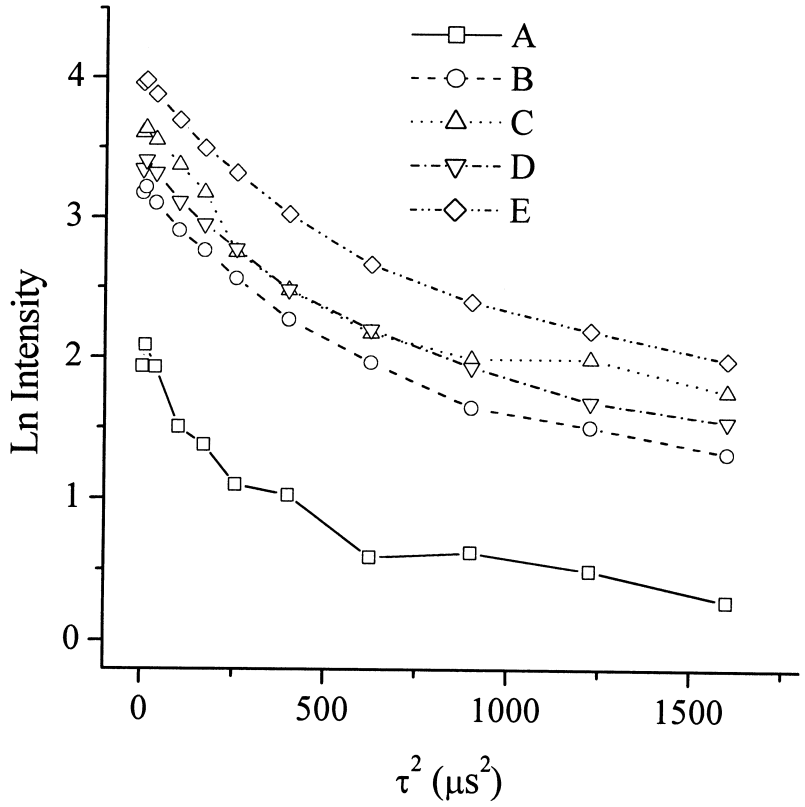


**FIGURE 9** Ln intensity of the $^{13}C$ CP/MAS spectra of the −0.52 ppm peak (-OsiCH$_3$) versus square of proton relaxation period $\tau^2$: (A) FPSI-25, (B) FPSI-35, (C) FPSI-50, (D) FPSI-75 and (E) FPSI-100.

and $T_2$ (slow), respectively. For each type of carbon, the y-axis intercepts in Figure 8 are proportional to the percentage of proton atoms to be found in each component (Table III). The fluorinated polyimide shows helix configurations due to the bending and twists of the polymer chain at -C(CF$_3$)$_2$- group in the AHHFP and 6FDA repeat unit. The flexible linkage of the trifluoromethyl group then separates the aromatic rings and hinders the interaction between neighboring molecules. Therefore, the configuration of FPI has a less packed structure, and its relaxation time (24.3 and 72.5 μs) is larger than that of FPSIs. For the imide segments in FPSIs, the fast ($11 \sim 18$ μs) and slow ($53 \sim 39$ μs) decaying components may be attributed to charge transfer complex and free imide

carbonyl, respectively. Moreover, the fraction of proton atoms in the former roughly increases with APrTMDS content. Interestingly, the structures of the FPSIs become more packed when incorporated with 20 mol % of APrTMDS into FPI, as observed from a comparison with the $T_2$ value (table III). However, the correlation between the ln $I$ of the $-0.52$ ppm peak (-OSi$\underline{C}$H$_3$) vs. the $\tau^2$ also exhibits two quasi-Gaussian decays (Figure 9). The relaxation times ($\sim 19$ and $\sim 43$ μs) and fraction of proton atoms are listed in Table III. The reason for the difference may be attributed also to charge-transfer complex configurations.

## CONCLUSIONS

A series of new hydroxyl-containing fluorinated poly(siloxane imide)s (FPSIs) were prepared from the reaction of 4,4′-(hexafluoroisopropylidene) diphthalic anhydride (6FDA) with 2,2′-bis(3-amino-4-hydroxyphenyl) hexafluoropropane (AHHFP) and 1,3-bis(3-aminopropyl)tetramethyl disiloxane (APrTMDS). FPSIs were characterized thorough IR, $^{13}$C-NMR, DSC and TGA. The incorporated flexible APrTMDS segments enhanced the degree of the imidization, reduced the acidity of the FPI polymer, and reduced the intermolecular interaction. The thermooxidative stability of AHHFP segments was enhanced as the APrTMDS segments incorporated, but the thermal stability was less affected. FPSIs containing more than 20% APrTMDS had the smaller spin-spin relaxation time $T_2$ than that of FPI, revealing that the FPSI had more packed configuration structure.



## REFERENCES

[1] Ghossh, M. K., and Mittal, K. L., eds. (1996). *Polyimide, Fundamentals and Applications*, Marcel Dekker, New York.
[2] Joly, C., Cerf, D. L., Chappey, C., Langevin, D., and Muller, G. (1999). *Sep. Pur. Tech.*, **16**, 47.
[3] Kim, J. H., Chang, B. J., Lee, S. B., and Kim, S. Y. (2000). *J. Membr. Sci.*, **169**, 185.
[4] Chen, T. A., Jen, A. K. Y., and Cai, Y. (1995). *J. Am. Chem. Soc.*, **117**, 7295.
[5] Trigaud, T., Moliton, J. P., Quillat, M., and Chiron, D. (1999). *Opt. Mater.*, **12**, 225.
[6] Kim, J. H., Kim, E. J., Choi, E. C., Kim, C. W., Cho, J. H., Lee, Y. W., You, B. G., Yi, S. Y., Lee, H. J., Han, K., Jang, W. H., Rhee, T. H., Lee, J. W., and Pearton, S. J. (1999). *Thin Solid Films*, **341**, 192.
[7] Belfield, K. D., Najjar, O., and Sriram, S. R. (2000). *Polymer*, **41**, 5011.
[8] Homma, T. (1995). *J. Noncryst. Solid*, **187**, 49.
[9] Lee, Y. K., and Murarka, S. P. (1999). *Mater. Res. Bull.*, **34**, 869.
[10] Ueda, M., and Nakayama, T. (1996). *Macromolecules*, **29**, 6427.
[11] Yu, H. S., Yamashita, T., and Horie, K. (1996). *Macromolecules*, **29**, 1144.
[12] Tullos, G. L., and Mathias, L. J. (1999). *Polymer*, **40**, 3643.
[13] Ricco, A. J., and Hoyt, A. E. (1995). *J. Am. Chem. Soc.*, **117**, 8672.

[14] Sun, H. T., Chen, Z. H., Wlodarski, W., and McCormick, M. (1996). *Sensors and Actuators B*, **35–36**, 146.
[15] Zheng, X. R., Lai, P. T., Liu, B. Y., Li, B., and Cheng, Y. C. (1997) *Sensors and Actuators A*, **63**, 147.
[16] Matsuguch, M., Kuroiwa, T., Miyagishi, T., Suzuki, S., Ogura, T., and Sakai, Y. (1998). *Sensors and Actuators B*, **52**, 53.
[17] Wessa, T., Barie, N., Rapp, M., and Ache, H. J. (1998). *Sensors and Actuators B*, **53**, 63.
[18] Grate, J. W., Kaganove, S. N., Patrash, S. J., Craig, R., and Bliss, M. (1997). *Chem. Mater.*, **9**, 1201.
[19] Grate, J. W., Patrash, S. J., Kaganove, S. N., and Wise, B. M. (1999). *Anal. Chem.*, **71**, 1033.
[20] Chang, T. C., and Wu, K. H. (1998). *Polym. Degrad. Stab.*, **60**, 161.
[21] Chang, T. C., Wu, K. H., and Chiu, Y. S. (1999). *Polym. Degrad. Stab.*, **63**, 103.
[22] Kuckertz, V. H. (1966). *Makromol. Chem.*, **98**, 101.
[23] Clair, A. K. S., Clair, T. L. S., and Shevket, K. I. (1984). *Polym. Mater. Sci. Eng.*, **51**, 61.
[24] Tékély, P., Canet, D., and Delpuech, J. (1989). *J. Mol. Phys.*, **67**, 81.
[25] Mikawa, M., Nagaoka, S., and Kawakami, H. (1999). *J. Membr. Sci.*, **163**, 176.
[26] Turk, M. J., Ansari, A. S., Alston, W. B., Gahn, G. S., Frimer, A. A., and Scheiman, D. A. (1999). *J. Polym. Sci. Part A: Polym. Chem.*, **37**, 3943.
[27] Molinero, A. L., Martinez, L., Villareal, A., and Castillo, J. R. (1998). *Talanta*, **45**, 1211.